IGSHPA Research Track
Las Vegas, December 6-8, 2022

Influence of buildings on geothermal boreholes – a comparison between two models.

Maria Letizia Fascì

ABSTRACT

The spread of ground source heat pumps has led to the development of several models to estimate the thermal interference between independent geothermal boreholes in densely populated areas. Some of these models take into account the changes in the ground surface temperature, thus allowing to account for the heat flux from the buildings, potentially high in densely populated areas. In this study, we investigated two models accounting for the ground surface temperature change; both models are based on the Stacked Finite Line Source (SFLS) model. The first model treats the ground surface as a set of rectangles, each with its own temperature; the second model treats the ground as an infinite surface with imposed temperature. The first model is more accurate, as it allows to consider different temperatures for different surfaces. However, the second model requires less computational time and is easier to implement. Therefore, we investigated whether the latter model can provide a good approximation of the former. Our results suggest that the second model can often provide a good approximation with significantly less computational time, especially for larger built areas; however, it could be unacceptably inaccurate for smaller neighbourhoods. We also investigated a strategy to improve its accuracy without compromising its computational speed; the strategy seems promising but requires more investigation.

INTRODUCTION

The increasing spread of Ground Source Heat Pumps (GSHPs), and thus the increasing number of areas characterized by a high density of these systems, has led to the development of several models and tools to calculate the thermal interference between neighbouring independent energy boreholes (Rivera et al. 2015; Fascì et al. 2021; Stockholms stad 2022; Witte 2018). Areas characterized by a high density of GSHPs are typically also characterized by a high density of buildings, responsible for the underground heat island effect, i.e., increased temperatures in the underground (Gunawardhana et al. 2011). Therefore, taking into account the heat island effect is potentially paramount for the accurate estimation of the operation of GSHPs, as this can increase the geothermal potential of areas with dominating heating demand and decrease the geothermal potential of areas with dominating cooling demand (Rivera et al. 2017).

Models to simulate the operation of energy boreholes accounting for the underground heat island effect have been proposed. They model the effect that temperature changes in the ground surface have on the underground assuming either a homogenous or a spatially variable change of the ground surface temperature (Rivera et al. 2015, Rivera et al. 2016, Fascì et al. 2022).

Maria Letizia Fascì (mlfasci@kth.se) is a PhD student at KTH - Royal Institute of Technology, Department of Energy Technology, Stockholm (Sweden).

DOI: https://doi.org/10.22488/okstate.22.000018

Since the ground surface is subject to different uses, e.g., buildings, asphalt, gardens, etc., and is thus characterized by local temperature changes, models that can account for a spatially variable ground surface temperature are more accurate. However, models that consider the ground surface as homogeneous, thus not considering the spatial variability of the ground usage, are easier to implement and computationally less demanding.

Therefore, in this paper, we investigate the accuracy of approximating the ground surface as a surface at uniform temperature rather than accounting for its spatial variability. We calculate the borehole wall temperatures in densely populated areas accounting for the effect of the boreholes operation and ground surface temperature. We compare the results obtained using two different models: a model that considers the spatial variability of the ground surface temperature and a model that considers the ground surface temperature as homogeneous. We evaluate the accuracy of the approximation for several synthetic scenarios and investigate a strategy to improve its accuracy.

METHODOLOGY

We have considered 18 scenarios (see section *Case studies*) and calculated the borehole wall temperature evolution during 50 years with the two models under research using a 1–year time resolution. We can use such a coarse time resolution compared to the 1-hour resolution often used for the study of GSHPs since we are comparing two models that differ in how they handle the effect of heat conduction from the ground surface to the borehole wall. This is a relatively slow phenomenon for which a 1-year resolution is sufficient, as shown for a comparable problem (Fascì et al, 2018). For all the scenarios, we have compared the two models by calculating the absolute and relative differences between the borehole wall temperature changes given by the models for each borehole and at each time step, i.e., the values:

$$\overline{\Delta T}_i^{\text{absolute}}(t) = |\overline{\Delta T}_i^{\text{FLS IV}_{\text{GST}^=}}(t) - \overline{\Delta T}_i^{\text{FLS IV}_{\text{GST}^\sim}}(t)| \quad (1)$$

and

$$\overline{\Delta T}_i^{\text{relative}}(t) = \frac{|\overline{\Delta T}_i^{\text{FLS IV}_{\text{GST}^=}}(t) - \overline{\Delta T}_i^{\text{FLS IV}_{\text{GST}^\sim}}(t)|}{\overline{\Delta T}_i^{\text{FLS IV}_{\text{GST}^=}}(t)} \quad (2)$$

where $\overline{\Delta T}_i^{\text{FLS IV}_{\text{GST}^=}}(t)$ and $\overline{\Delta T}_i^{\text{FLS IV}_{\text{GST}^\sim}}(t)$ are the wall temperature change of the borehole *i* at time *t* calculated with the models $\text{FLS IV}_{\text{GST}^=}$ and $\text{FLS IV}_{\text{GST}^\sim}$ respectively (details about the models are given in the section *Models*).

Then, we have investigated a strategy to decrease the difference between the models. This strategy is described in the subsection $FLS\ IV_{GST^\sim}$.

Models

The models we have compared are based on the strategy described by Fascì et al. (2022). Each borehole is modelled as a set of 12 stacked segments on top of each other, so that it is possible to impose a uniform borehole wall temperature along the boreholes (Cimmino, 2014). The depth-averaged temperature $\overline{T}_{i,j}(t)$ on each borehole segment *i,j* at time *t* is calculated as the sum of :

- the initial depth-averaged undisturbed ground temperature $\overline{T}_{i,j}^{IC}$;
- the depth-averaged ground temperature change induced on the borehole segment by the heat extraction/rejection of all the boreholes in the area $\overline{\Delta T}_{i,j}^{BHEs}(t)$
- the depth-averaged temperature change induced on the borehole segment by changes in the ground surface temperature compared to the initial condition $\overline{\Delta T}_{i,j}^{TBC}(t)$:

$$\overline{T}_{i,j}(t) = \overline{T}_{i,j}^{IC} + \overline{\Delta T}_{i,j}^{BHEs}(t) + \overline{\Delta T}_{i,j}^{TBC}(t) \quad (3)$$

In this study we have assumed the undisturbed temperature uniform throughout the ground, i.e.:

$$\overline{T}_{i,j}^{IC} = \overline{T}^{IC} \quad \forall \text{ borehole segment } i,j \tag{4}$$

The term $\overline{\Delta T}_{i,j}^{BHEs}(t)$ is calculated using the Finite Line Source (FLS) model (Spitler and Bernier, 2016). The term $\overline{\Delta T}_{i,j}^{TBC}(t)$ is calculated in two different ways depending on the model adopted: whether the model accounts for the spatial variability of the ground surface temperature or not. We will refer to the two models as the "accurate model" and "approximated model" respectively. We will also refer to them with the acronyms $\text{FLS IV}_{\text{GST}=}$ and $\text{FLS IV}_{\text{GST}\sim}$ respectively. Details on the calculation of $\overline{\Delta T}_{i,j}^{TBC}(t)$ are given in the following subsections.

Writing equation 3 for each borehole segment we can calculate all the borehole wall temperatures in an area. For more details on the complete model we refer to Fascì et al. (2022).

$\text{FLS IV}_{\text{GST}=}$. Our formula to calculate $\overline{\Delta T}_{i,j}^{TBC}$ with the accurate model is an extension of the formula given by Rivera et al. (2017). $\overline{\Delta T}_{i,j}^{TBC}$ is calculated as:

$$\overline{\Delta T}_{i,j}^{TBC}(t) = \frac{1}{8\, H_{i,j}\sqrt{\pi}}\left[(H_{i,j} + D_{i,j}) \cdot f(H_{i,j} + D_{i,j}, t) - D_{i,j} \cdot f(D_{i,j}, t)\right] \tag{5}$$

where $H_{i,j}$ and $D_{i,j}$ are respectively the length and buried depth of the borehole segment *i,j*; the function *f* is calculated as:

$$f(z,t) = \sum_{k=1}^{n_{surf}} \Delta T_{GST}^{k} \int_{\frac{z^2}{4\alpha t}}^{\infty} \frac{1-e^{-u}}{u^{3/2}} \left[\text{erf}\left(\frac{y_i - y_b^k}{z}\sqrt{u}\right) - \text{erf}\left(\frac{y_i - y_a^k}{z}\sqrt{u}\right)\right]\left[\text{erf}\left(\frac{x_i - x_b^k}{z}\sqrt{u}\right) - \text{erf}\left(\frac{x_i - x_a^k}{z}\sqrt{u}\right)\right] du \tag{6}$$

where n_{surf} is the number of ground surfaces on which the temperature changes compared to the initial condition, e.g., the number of buildings; ΔT_{GST}^{k} is the ground surface temperature change of the *k-th* surface; α is the ground thermal diffusivity; x_i and y_i are the coordinates of the *i-th* borehole; x_a^k, x_b^k, y_a^k, y_b^k are the coordinates delimiting the *k-th* surface; *erf* is the error function (Andrews, L.C. 1998). One may notice that in equation 6 the term ΔT_{GST}^{k} is treated as a constant and appears outside of the integral, while in the original formulation by Rivera et al. (2017) ΔT_{GST}^{k} is expressed as a function of time and therefore appears inside the integral. We could have left this term inside the integral for the sake of generalizability, however, since our methodology is tailored to the built environments, where we assume the ground surface temperature below the buildings to be constant, we have moved the term outside of the integral. We will also refer to the term ΔT_{GST}^{k} as the ground temperature change below the *k-th* building.

$\text{FLS IV}_{\text{GST}\sim}$. The approximated model calculates $\overline{\Delta T}_{i,j}^{TBC}$ as in Fascì et al. (2022):

$$\overline{\Delta T}_{i,j}^{TBC}(t) = \frac{\Delta T_{GST}}{H_{i,j}}\left[(H_{i,j} + D_{i,j}) \cdot g(H_{i,j} + D_{i,j}, t) - D_{i,j} \cdot g(D_{i,j}, t)\right] \tag{7}$$

with:

$$g(z,t) = \left\{ \text{erf}\left(-\frac{z}{\sqrt{4\alpha t}}\right) + \sqrt{\frac{4\alpha t}{\pi z^2}}\left(1 - e^{-\frac{z^2}{4\alpha t}}\right) + 1 \right\} \tag{8}$$

where ΔT_{GST} is the ground surface temperature change, considered uniform along the infinite ground surface. When calculating the borehole wall temperatures by using $\text{FLS IV}_{\text{GST}\sim}$, we have considered:

$$\Delta T_{GST} = \frac{\cancel{A^0 \cdot \Delta T_{GST}^0} + \sum_{k=1}^{n_{surf}} \Delta T_{GST}^{k} \cdot A^k}{A^0 + \sum_{k=1}^{n_{surf}} A^k} \tag{9}$$

i.e., the ground surface temperature change on the uniform infinite surface is equal to the weighted average between the ground surface temperature change below the buildings - ΔT_{GST}^{k}- and the ground surface temperature change in the area delimited by the buildings - ΔT_{GST}^{0}- (Figure 1). Since we assume that ΔT_{GST}^{0} = 0 K we have cancelled the term $A^0 \cdot \Delta T_{GST}^{0}$

in equation 9. We will refer to this model as the "basic FLS $IV_{GST\sim}$".

We have then evaluated the possibility to minimize the difference between the models by an optimal choice of ΔT_{GST}:

$$\Delta T_{GST} = \frac{\sum_{k=1}^{n_{surf}} \Delta T_{GST}^{k} \cdot A^{k}}{c\,(A^{0} + \sum_{k=1}^{n_{surf}} A^{k})} \tag{10}$$

where c is a multiplication factor we calculated for each scenario by minimizing the Root Mean Square Error (RMSE) between FLS $IV_{GST=}$ and FLS $IV_{GST\sim}$, i.e., where c is such that:

$$\sqrt{\frac{1}{50 \cdot n_{boreholes}} \sum_{t=1\,year}^{t=50\,years} \sum_{i=1}^{n_{boreholes}} \overline{(\Delta T_i^{FLS\ IV_{GST=}}(t) - \overline{\Delta T_i}^{FLS\ IV_{GST\sim}}(t,c))^2}} \tag{11}$$

is minimum. We will refer to this model as to the "optimized FLS $IV_{GST\sim}$".

Scenarios

We have studied areas with boreholes positioned in square grids. We have considered the number of boreholes per side equal to N = 2, 3… 10; the total number of boreholes in an area is equal to $n_{boreholes} = N^2$. Each borehole is centred on a house of area 10 x 10 m². We have assumed that the ground surface temperature change below the houses is 7 K, otherwise 0 K. We have considered grids characterized by borehole distances B_1 = 15 m and B_2 = 20 m. The scenario with N= 2 and B = 20 m is shown as an example (Figure 1).

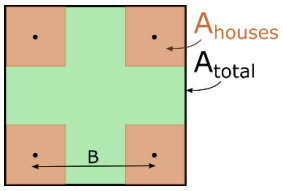

Figure 1 Map of the case study with N = 2, B = 20 m.The ground properties used for the simulations are shown in Table 1. The borehole properties are shown in Table 2.

Table 1. Ground Properties

Undisturbed temperature T_o [°C]	Thermal conductivity k [W/mK]	Thermal diffusivity α [m²/s]
8.0	3.1	$1.55 \cdot 10^{-6}$

Table 2. Boreholes Properties

Radius [m]	Buried depth [m]	Length [m]	Constant linear heat load [W/m]
0.0575	6	200	-15 (extraction)

RESULTS AND DISCUSSION

We show the results for the central and corner boreholes of our scenarios. The central boreholes correspond to the one borehole at the centre of the area when N is odd, and to the four boreholes at the center of the area when N is even; the corner boreholes are always four. The cases for N =3 and N = 4 are shown in Figure 2 as an example.

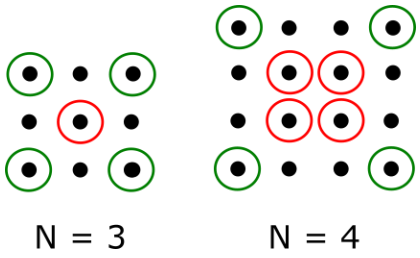

Figure 2 Central (red circles) and corner (green circles) boreholes in the scenarios with N = 3 and N = 4.

The temperature evolutions calculated with FLS $IV_{GST=}$ and the basic FLS $IV_{GST\sim}$ for the central and corner boreholes of the scenarios with B = 15 m are shown in Figure 3 for the cases N = 2 and N = 10. Details about the differences between the two models are given in Table 3 and Table 4 for all values of N considered.

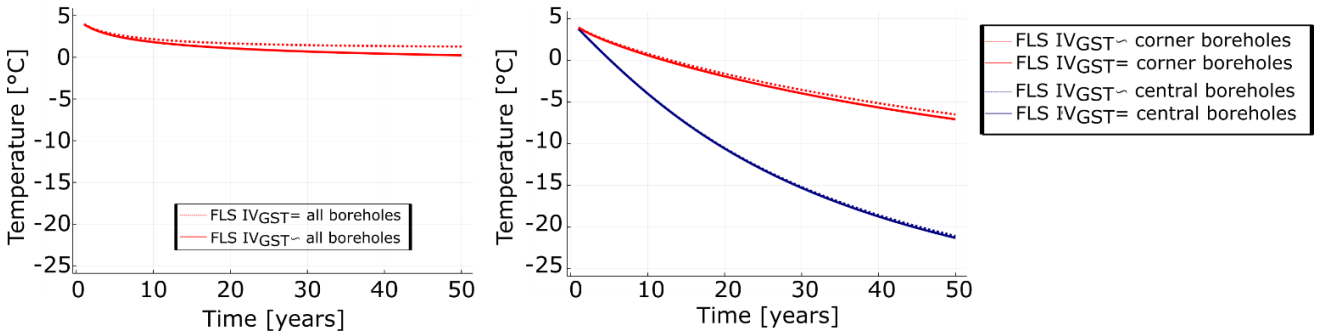

Figure 3 Temperature evolutions of the corner and central boreholes for the scenarios with B = 15 m and N = 2 (left), N = 10 (right).

Table 3. Difference Between FLS $IV_{GST=}$ and FLS $IV_{GST\sim}$ @ t = 10 Years for B = 15 m

		N = 2	N = 3	N = 4	N = 5	N = 6	N = 7	N = 8	N = 9	N =10
Central BHE	**Absolute [K]**	0,35	0,22	0,15	0,10	0,07	0,05	0,036	0,026	0,021
	Relative [%]	5,6	2,6	1,6	0,92	0,65	0,41	0,30	0,22	0,17
Corner BHE	**Absolute [K]**	0,35	0,26	0,23	0,21	0,20	0,19	0,19	0,18	0,18
	Relative [%]	5,6	3,8	3,2	2,9	2,7	2,6	2,6	2,5	2,5

The results show that the difference between the models is higher for smaller neighbourhoods and increases with time both in absolute and relative terms. For example, after 10 years of operation, the results between the models differ by 5,6% for the boreholes of the smallest neighbourhood (N = 2) and by 2,5% for the corner boreholes of the biggest neighbourhood (N =10). The differences increase to 14% and 3,9% respectively after 50 years. It can also be noticed that the difference between the models is smaller for the central boreholes than the corner boreholes. For example, after 50 years, the difference for the central boreholes of the biggest neighbourhood is 0,78%, the difference for the corner boreholes of the same neighbourhood is 3,9%.

Table 4. Difference Between FLS $IV_{GST=}$ and FLS $IV_{GST\sim}$ @ t = 50 Years for B = 15 m

		N = 2	N = 3	N = 4	N = 5	N = 6	N = 7	N = 8	N = 9	N =10
Central BHE	Absolute [K]	1,1	0,82	0,69	0,57	0,48	0,40	0,33	0,27	0,23
	Relative [%]	14	7,0	4,7	3,1	2,3	1,7	1,3	0,97	0,78
Corner BHE	Absolute [K]	1,1	0,87	0,77	0,71	0,66	0,63	0,61	0,60	0,59
	Relative [%]	14	8,7	6,6	5,4	4,8	4,4	4,2	4,0	3,9

The temperature evolutions calculated with FLS $IV_{GST=}$ and the basic FLS $IV_{GST\sim}$ for the central and corner boreholes of the scenarios with B = 20 m are shown in Figure 4 for the cases N = 2 and N = 10. Details about the differences between the two models are given in Table 5 and Table 6 for all values of N considered.

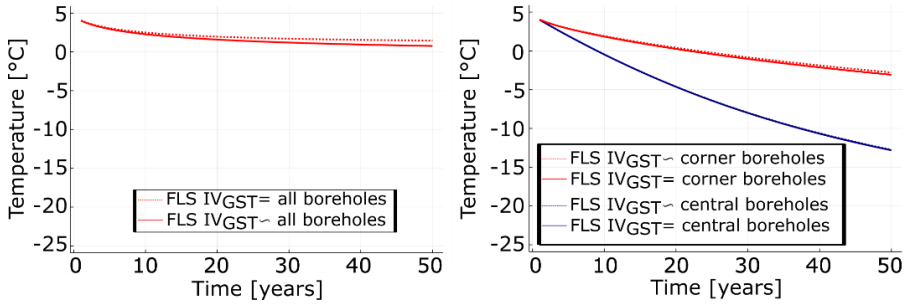

Figure 4 Temperature evolutions of the corner and central boreholes for the scenarios with B = 20 m and N = 2 (left), N = 10 (right).

Table 5. Difference Between FLS $IV_{GST=}$ and FLS $IV_{GST\sim}$ @ t = 10 Years for B = 20 m

		N = 2	N = 3	N = 4	N = 5	N = 6	N = 7	N = 8	N = 9	N =10
Central BHE	Absolute [K]	0,22	0,11	0,07	0,038	0,025	0,015	0,009	0,0053	0,0025
	Relative [%]	3,84	1,54	0,90	0,46	0,30	0,17	0,11	0,062	0,0297
Corner BHE	Absolute [K]	0,22	0,15	0,12	0,10	0,096	0,09	0,086	0,083	0,080
	Relative [%]	3,84	2,41	1,9	1,7	1,55	1,46	1,39	1,34	1,30

Table 6. Difference Between FLS $IV_{GST=}$ and FLS $IV_{GST\sim}$ @ t = 50 Years for B = 20 m

		N = 2	N = 3	N = 4	N = 5	N = 6	N = 7	N = 8	N = 9	N =10
Central BHE	Absolute [K]	0,70	0,47	0,36	0,27	0,21	0,16	0,12	0,090	0,069
	Relative [%]	9,67	4,56	2,90	1,81	1,29	0,87	0,65	0,45	0,33
Corner BHE	Absolute [K]	0,70	0,51	0,43	0,38	0,35	0,33	0,32	0,31	0,298
	Relative [%]	9,67	5,83	4,36	3,6	3,2	3,0	2,86	2,76	2,69

The results for the scenarios with B = 20 m confirm the trends observed for the scenarios with B =15 m. Moreover, these results show that the difference between the models is lower for higher values of B. For example, the difference between the models for the smallest neighbourhood after 50 years is 14% when B =15 m and 9,7% when B = 20 m; for the corner boreholes in the biggest neighbourhood, the difference after 50 years is 3,9% when B = 15 am and 2,7% when B = 20. However, we believe that the difference between the models has a non-monotone trend with B since for $B \rightarrow \infty$ the value ΔT_{GST} used by the approximated model tends to 0, neglecting the presence of the houses. More investigation is needed to confirm the trend of the difference with B.

Overall, our simulations show that the difference between the two models can often be considered acceptable, being lower than 3% and 6% after respectively 10 and 50 years for all the boreholes in 14 out of the 18 scenarios studied. However, the difference between the models could be considered unacceptable for smaller neighbourhoods for which we have calculated differences of up to 14%.

From the results, we notice that despite the heat losses from the buildings, the borehole wall temperature decreases monotonously. This result is specifically related to the case studies analysed, where the heat losses from the buildings do not compensate the heat extraction form the boreholes. The borehole wall temperature trend could be different for different scenarios. Another observation is that in some cases the borehole wall temperature decreases below – 12 °C. While this is possible in our simulations where we imposed a constant heat extraction from the ground for 50 years, in reality, heat pumps typically turn off when the inlet brine temperature decreases below -7°C/-12 °C, limiting the ground temperature decrease.

Figure 5 shows the computational time for our scenarios. We want to point out that we did not perform a proper benchmarking and the results might be slightly affected by the use of the computer for other purposes. Moreover, although our scenarios present symmetries, these are not exploited so that comparable results can be expected for real scenarios, typically not presenting many symmetries. The results were obtained with a computer equipped with a Intel(R) Core(TM) i7-7600U processor (2.8 GHz) and 32 Gb of RAM.

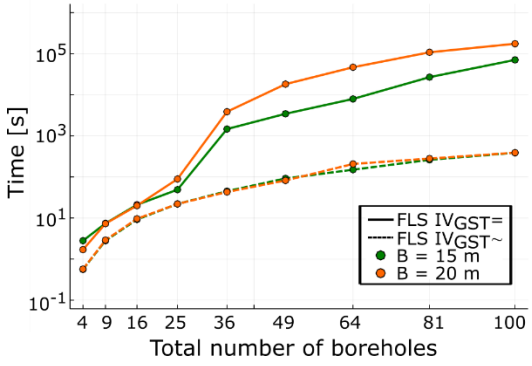

Figure 5 Computational time of our scenarios.

Figure 5 shows that the computational time of the accurate model is relatively low for the smaller neighbourhoods – for which the approximated model is less accurate -, and significantly higher for the bigger neighbourhoods – for which the approximated model is more accurate. Therefore, we suggest the use of the accurate model for the smaller neighbourhoods and of the approximated model for the bigger neighbourhoods. As a rule of thumb, we suggest to use the accurate model for neighbourhoods with less than 25 buildings, given the sharp increase in computational time for bigger neighbourhoods. We believe that the sharp increase in computational time for bigger neighbourhoods may be due to the influence of many buildings being negligible for many boreholes when the neighbourhood is bigger; therefore, the result of the integral in equation 6 being close to 0 for many computations. In fact, we had noticed in the past that the numerical computation of integrals close to 0 can be more expensive (Fascì et al, 2019). However, we have not analysed this further.

The multiplication factors obtained for the optimized FLS $IV_{GST\sim}$ and the RMSE of the optimized FLS $IV_{GST\sim}$ are shown in Figure 6.

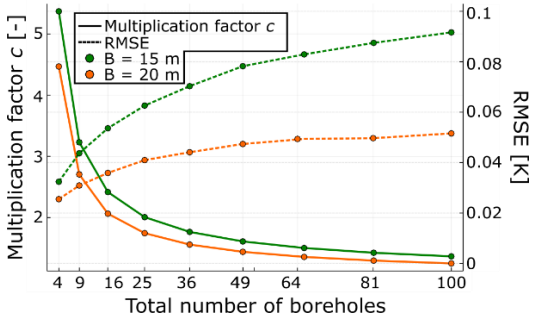

Figure 6 Multiplication factors c and root mean square errors of the optimized FLS $IV_{GST\sim}$

The multiplication factor decreases as the size of the neighbourhood increases. This is consistent with the previous results showing that the basic FLS $IV_{GST\sim}$ is more accurate for bigger neighbourhoods. It is also higher for the scenarios with B =15 m than for B = 20 m. This is also consistent with the previously discussed results. The optimized FLS $IV_{GST\sim}$ is significantly more accurate than its basic version. In fact, the maximum RMSE calculated with the optimized FLS $IV_{GST\sim}$ is lower than 0.1 K in opposition to the maximum RMSE of the basic FLS $IV_{GST\sim}$ - 0.5 K-. One may also notice that while the basic FLS $IV_{GST\sim}$ is most accurate with bigger neighbourhoods, the optimized FLS $IV_{GST\sim}$ is most accurate with smaller neighbourhoods.

Although optimizing FLS $IV_{GST\sim}$ increases significantly the accuracy of the model, the calculation of the multiplication factors c requires the use of FLS $IV_{GST=}$, making the model pointless. More investigation is needed to understand if a correlation between the multiplication factors and other characteristics of the neighbourhood or precalculated multiplication factors can be found and to extend the results to areas characterized by an irregular distribution of boreholes and houses.

CONCLUSION

We have compared two models to calculate the borehole wall temperature evolutions in densely populated areas taking into account the thermal impact of the buildings on the underground. One of the models - FLS $IV_{GST=}$ - is more accurate but computationally more demanding, while the other - FLS $IV_{GST\sim}$ - is an approximation of the first and computationally cheaper. We have showed that FLS $IV_{GST\sim}$ tends to be a good approximation of FLS $IV_{GST=}$ for bigger neighbourhoods, but is less accurate for smaller neighbourhoods. We have also initiated the investigation of a strategy to improve the accuracy of FLS $IV_{GST\sim}$ without reducing its speed. The resulting "optimized" FLS $IV_{GST\sim}$ is a good approximation of FLS $IV_{GST=}$ even for smaller neighbourhoods.

This study analysed several case studies, however, we believe that more should be analysed to draw generalised conclusions and understand the effect of several parameters not analysed in this article, like the boreholes length and the relative position between boreholes and houses.

ACKNOWLEDGMENTS

This project is supported by the Swedish Energy Agency under grant P43647-3. The project is carried on in partnership with Bengt Dahlgren Geoenergi, Borrföretagen i Sverige, Neoenergy Sweden, Nibe, Nowab, Stockholms stad, Svenskt Geoenergicentrum, Thermia and Täby kommun.

REFERENCES

Andrews, L. C. 1998. *Special functions of mathematics for engineers.* SPIE Press.

Cimmino, M., and M. Bernier. 2014. *A semi-analytical method to generate g-functions for geothermal bore fields. International Journal of* Heat and Mass Transfer 70: 641-650.

Fascì, M. L., A. Lazzarotto, J. Acuna, and J. Claesson. 2018. *Thermal influence of neighbouring GSHP installations: Relevance of heat load temporal resolution.* Proceedings of the IGSHPA Research Track 2018

Fascì, M. L., A. Lazzarotto, J. Acuña, and J. Claesson. 2019. *Analysis of the thermal interference between ground source heat pump systems in dense neighbourhoods.* Science and Technology for the Built Environment 25: 1069-1080.

Fascì, M. L., A. Lazzarotto, J. Acuña, and J. Claesson. 2021. *Simulation of thermal influence between independent geothermal boreholes in densely populated areas.* Applied Thermal Engineering, 196, 117241.

Fascì, M. L., W. Mazzotti, A. Lazzarotto, and J. Claesson. 2022. *Temperature of Energy Boreholes Accounting for Climate Change and the Built Environment - a New Model for its Estimation.* SSRN preprint 4113861.

Gunawardhana, L. N., S. Kazama, and S. Kawagoe. 2011. *Impact of urbanization and climate change on acquifer thermal regimes.* Water resources management 25.13: 3247-3276.

Rivera , J. A., P. Blum, and P. Bayer. 2015. *Analytical simulation of groundwater flow and land surface effects on thermal plume of borehole heat exchangers.* Applied Energy 146: 421-433.

Rivera, J. A., P. Blum, and P. Bayer. 2016. *Influence of spatially variable ground heat flux on closed-loop geothermal systems: Line source model with nonhomogeneous Cauchy-type boundary conditions.* Applied Energy 180: 572-585.

Rivera, J. A., P. Blum, and P. Bayer, 2017. *Increased ground temperatures in urban areas: estimation of the technical geothermal potential.* Renewable Energy 103: 388-400.

Spitler, J. D., and M. Bernier. 2016. *Vertical borehole ground heat exchanger design methods.* In Advances in Ground-Source Heat Pump Systems. S.J. Rees, ed.London: Woodhead Publishing.

Stockholm stad. 2022/06/09. *Beräkningsprogram för dimensionering av energibrunnar*. Retrieved from https://boende.stockholm/siteassets/mitt-boende/blanketter/miljoforvaltningen/varmepumpar/om-berakningsprogram-for-dimensionering-av-energibrunnar.pdf

Witte, H. J. 2018. *A novel tool for assessing negative temperature interactions between neighbouring borehole heat exchanger systems.* 14th International Conference on Energy Storage - EnerSTOCK 2018.